2023-24-0159

Experimental and numerical electro-thermal characterization of lithium-ion cells for vehicle battery pack applications

Author, co-author (Do NOT enter this information. It will be pulled from participant tab in MyTechZone)

Affiliation (Do NOT enter this information. It will be pulled from participant tab in MyTechZone)

Abstract

Batteries are the key elements for the massive electrification of the transport sector. With the rapidly growing popularity of electric vehicles, it is becoming increasingly important to characterize the behavior of battery packs through fast and accurate numerical models, in order to support experimental activities. A coupled electro-thermal simulation framework is required, as it is the only way to realistically represent the interactions between real world battery pack performances and the vehicle-level thermal management strategies. The purpose of this work is to pave the way for a comprehensive methodology for the development of a supporting modeling framework, to efficiently complement experiments in the optimal design and integration of battery packs.
The full methodology consists of the following steps: i) an experimental analysis of the temperature and current dependence on various internal parameters of selected lithium-ion cells based on their electrochemical properties, ii) development and implementation of a battery cell electric model that takes into account the aforementioned dynamics and their dependencies; the electrical model is based on the Equivalent Circuit Model (ECM) and can be used to calculate the electrical output and losses of Li-ion cells as a function of state of charge and current; iii) development of a cell-level multi-domain computational framework for coupled electro-thermal simulations, based on state-of-the art CFD software tools; iv) validation and tuning of the multi-domain framework through ad-hoc designed experiments with controlled cell charge-discharge profiles and temperature measurement; v) extension of both the ECM and multi-domain approaches to full-scale battery packs, to be adopted for electric vehicle characterization under realistic driving conditions, with detailed battery thermal management.
Results shown in the present paper cover steps i) to iv) and include a series of static and dynamic experimental tests with voltage response and temperature measurements performed on the selected Li-ion cells. It is shown that the proposed modeling tools can accurately predict the electro-thermal behavior of the cells under static and dynamic current conditions. Most of the average relative errors between predicted values and test values obtained do not exceed 10%.

Introduction

Electric vehicles and stationary energy storage make extensive use of lithium-ion batteries (Li-ions), which are crucial to the decarbonization of the transportation and energy industries [1]. In order to guarantee both safety and effectiveness, the real-time operation of the battery system must be monitored and controlled by a battery management system (BMS). A battery model is typically required to predict the dynamics of the system under various operating conditions in order to improve the functionality of the BMS [2].

Among different types of models, including electrochemical models, reduced order models and black-box models the equivalent circuit model (ECM) has been widely used for model-based real-time parameter and state estimation of Li-ions [3].

Improving the ECM's accuracy is important for the BMS and the battery system. First, a high ECM accuracy leads to accurate prediction of the battery's power capacity, which is a key parameter for real-time power management of the battery system, e.g.

during EV's operation. Second, the ECM accuracy affects the estimation accuracy of the battery's internal power loss and heat generation, as well as the resulting temperature rise, which is key to ensuring proper thermal management [4].

Furthermore, alongside with fast and efficient electrical models, it is crucial to develop detailed multi-dimensional thermal modeling frameworks, to assist battery pack optimal design and the integration of the battery pack with the system-level thermal management.

Within the context described above, the contribution of the present work can be summarized as: i) an experimental characterization of selected 21700 Li-ion cells with comparable nominal energy densities and chemistries, in terms of current-voltage-temperature dependence; ii) development and implementation of an ECM-based battery cell electric model, with the aim of capturing the aforementioned dynamics and their dependencies; the electrical model is intended to calculate the electrical output and losses of Li-ion cells as a function of state of charge and current; iii) development, calibration and testing of a cell-level computational approach for the detailed thermal behavior analysis of Li-ion cells, based on the state-of-the art ANSYS® Fluent CFD package.
The remainder of the paper is organized as follows: first, in the Materials and methods section, the experimental setup and test schedule are described, followed by the presentation of the electrical and thermal modeling framework and the related preliminary calibration activity. After that, the main results and findings from the comparison between models and experiments are shown in the Results and discussion section. Final remarks and suggestions for future developments are included in the Conclusions section.

Materials and methods

Battery experimental setup

The battery test platform includes the bi-directional IT6000C series programmable DC tester, computer for user-machine interface and data storage, a switch board for cable connection, and the battery cells. The bi-directional programmable DC power supply combines two functions in one: source and sink with energy regeneration. The platform is capable of charge–discharge exposed in battery modules with a maximum voltage of 80 V at the frequency of 50/60 Hz and the maximum current is 150 A and power of 5 kW. ITS5000 Test System software provides the users with an array of charge/discharge modes such as CC/CP/CR discharge mode and it can simulate constant voltage charge and constant current charge modes. Temperatures of the cells are measured with PT100 temperature sensors clamped on the cell case. All experiments are performed at room temperature. National Instruments FP-RTD-122 module is used for battery surface temperature monitoring. During the charging/discharging, voltage, current, temperature of each cell is measured and recorded at a rate of one sample per second.

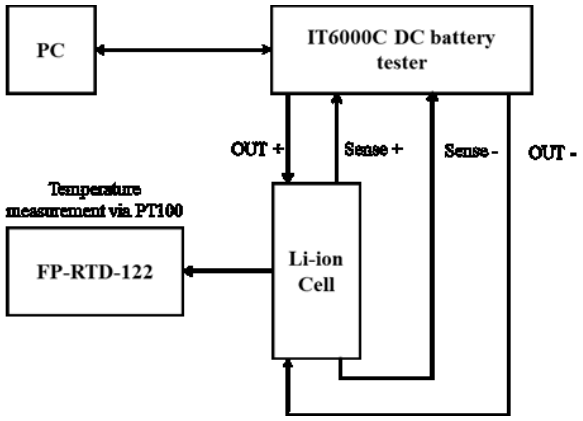

Figure 1. Schematic of the measurement circuit for the lithium-ion cells with battery testing system.

Battery test schedule

Three types of cylindrical lithium nickel–manganese–cobalt oxide (LiNMC) cells are selected for cycle tests. They are: 1. INR21700-M50LT, 2. INR21700-50E and 3. INR21700-40T. Their key specifications are shown in Table 1.

Table 1. Overview of cells investigated in this study

Cell	INR21700-M50LT	INR21700-50E	INR21700-40T
Origin	commercial	commercial	commercial
Chemistry	NMC	NMC	NMC
Vmin:Vmax [V]	2.5:4.2	2.5:4.2	2.5:4.2
Nominal capacity [Ah]	4.89	5	4

Geometry	cylindrical	cylindrical	cylindrical
D*H [mm]	21.1*70.2	20.3*70.8	21.0*70.1
Mass [g]	68.2	69.0	67.0

Two types of cell tests were performed to characterize the cell tested in this work. The first type comprised a constant current discharge and charge tests. The selected cell types are discharged each with 1C, 3C and 5C current to the discharge voltage limit specified by the cell manufacturer. The discharge and charge parameters are listed in Table 2. The experimental data, i.e. voltage and surface temperature distributions profiles during different C-rate discharge rates, obtained from static tests were used to verify and validate the thermal and electric simulation models. The voltage, profiles for theses tests are presented in Figure 2 (a), (b) and (c).

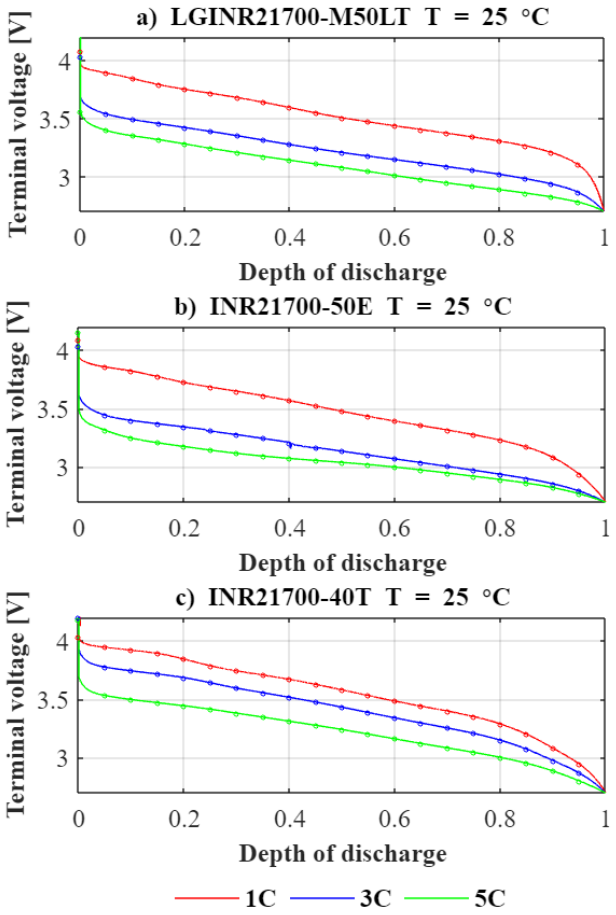

Figure 2. Plots showing SOC vs. terminal voltage a) 1 battery, b) 2 battery, c) 3 battery during static discharge at environmental temperature of 25°C.

The second type comprised a sequence of constant-current discharge pulses. Discharge pulses of 1C were used. Between two adjacent test points in each characterization test the cells are charged or discharged to reach the desirable initial SOC values and rested of 120 min in each case to reach an electrical, chemical and thermal equilibrium condition [5], [6]. The voltage, current and SOC profiles for this test are presented in Figure 3 (a), (b) and (c).

Table 2. Charging and discharging parameters of the cycle test.

Cell	INR21700-M50LT	INR21700-50E	INR21700-40T
Charging rate	1C	1C	1C
Discharging rate	1C,3C,3C	1C,3C,3C	1C,3C,3C
Charging cut-off voltage	4.2	4.2	4.2
Discharging cut-off voltage	2.7	2.7	2.7

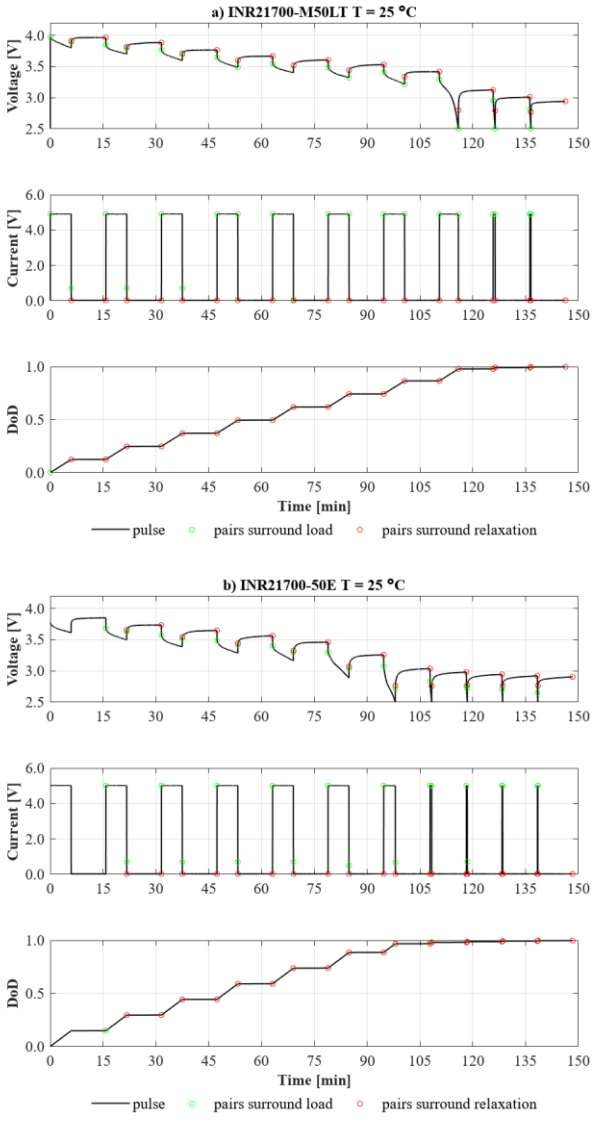

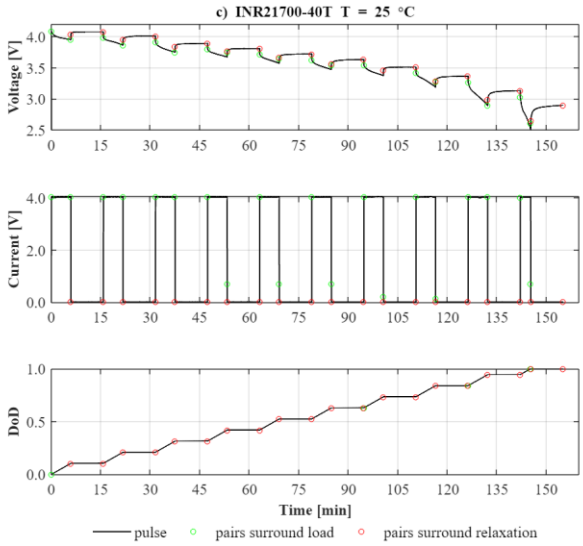

Figure 3. Plots showing voltage, current and DoD vs. time for pulsed-current cell tests for the a) LGINR21700-M50LT, b) INR21700-50E and c) INR21700-40T cells during pulse discharge and environmental temperature of 25°C.

The datasets collected in the pulse characterization tests were used for the identification of model parameters and comparison in this paper, described in the next sections. The goal is to have the cell model output resemble the cell terminal voltage under load as closely as possible, at all times, when the cell model input is equal to the cell current.

Modeling framework

Electric model structure

A modelling approach based on equivalent circuit model (ECM) with n RC network is proposed to predict the battery electric performance characteristics [3]. In this study, the ECM uses parameters derived from experimental electrochemical characterizations, such pulse charge and discharge curves [2], [6], [7]. The effects of battery SOC and current are covered explicitly in these models. In this study, however, the effect of ambient temperature is not captured. The ECM model is composed of three modules [7]: 1) the open circuit voltage module v_{OCV}, 2) the internal resistance module R_0 and 3) the RC network module.

The basic definition of SOC, battery model, and parameter identification algorithm are introduced first.

The structure of the proposed model is shown in Figure 4 where v_{OCV} indicates the open circuit voltage, v_T and i represent the battery terminal voltage and current (positive for charging and negative for discharging), respectively. T represents the ambient temperature. Denote n as the number of RC networks. R_0 is the ohmic internal resistance, R_n are the polarization internal resistances, and C_n are the polarization capacitances.

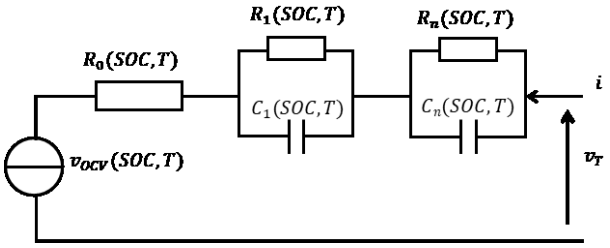

Figure 4. Schematic diagram of SOC and temperature dependent battery ECM

Let define $i_j, v_j, j = 1,2,\dots,n$, as the current and overpotential across R_j. Assuming the RC parameters and the constant current between two data samples, where Δt is the sampling interval in seconds, k is the sample time and τ_j is the time constant, the dynamics of the RC networks in discrete form can be formulated as follows:

$$v_j[k+1] = a_j v_j[k] + R_j(1-a_j)i[k], j = 1,2,\dots,n \quad (1)$$

where $\left(\frac{-\Delta t}{\tau_j}\right)$ and $\tau_j = R_j C_j$

Further, the total voltage drop across all the RC networks can be expressed as:

$$v_{RC}[k] = \sum_{j=1}^{n} v_j[k] \quad (2)$$

The battery SOC and DOD are obtained using the widely employed coulomb counting method [9], [32]:

$$SOC[k+1] = SOC[k] + \frac{\Delta t}{3600Q}\eta_b[k]i[k] \quad (3)$$

and $$DOD[k] = 1 - SOC[k]$$

where Q in Ah the battery's nominal capacity at 25 °C and η_b is battery efficiency. Finally, the battery terminal voltage can be expressed as:

$$v_t[k] = v_{OCV}[k] + R_0[k]i[k] + v_{RC}[k] \quad (4)$$

The parameters to be identified are R_0 , R_n, C_n and v_{OCV}. The proposed method for ECM parameter identification considers the estimation of the resistance and capacitance values, as well as the

battery v_{OCV} along the SOC breakpoints between 0% and 100%, based on the pulse discharge tests presented in Figure 3. Each pulse provided separate information about v_{OCV}, R_0 and the circuit transients R_n and C_n. Based on the data in Figure 3 containing discharge pulses for each battery, the corresponding values of SOC that occurred before and after each pulse were determined. Further, the values of each circuit element were represented with lookup table versus the points of SOC.
The estimation technique implemented curve fitting procedure using a linear system and optimization approaches, pulse-by-pulse.
Model fit was judged by comparing root-mean-squared estimation error (estimation error equals cell voltage minus model voltage). In this paper, it was considered just one ambient temperature and one discharge current (1C).

Thermal model structure and validation

For the detailed thermal modeling of the tested battery cells, the ANSYS® Fluent CFD package is adopted. The underlying approach is called Multi-Scale Multi-Domain method [8], [9] and it requires the solution on a finite-volume grid of the following differential equations:

$$\frac{\partial \rho C_p T}{\partial t} - \nabla \cdot (\lambda \nabla T) = \sigma_+ |\nabla \phi_+|^2 + \sigma_- |\nabla \phi_-|^2 + S_{th} \quad (5)$$

$$\nabla \cdot (\sigma_+ \nabla \phi_+) = -S_{el} \quad (6)$$

$$\nabla \cdot (\sigma_- \nabla \phi_-) = S_{el} \quad (7)$$

where ϕ_+, ϕ_- are phase potentials for the positive and negative electrodes, with σ_+, σ_- being their effective electric conductivities, respectively. The terms S_{th} and S_{el} represent thermal and electrical source terms, which might be related to electrochemistry, internal short-circuit and/or thermal abuse [8]. For the purposes of the present work, the source terms were evaluated through a polynomial fitting procedure [10], which allows to directly import experimental discharge curves including also environmental temperature effects. More in details, S_{el} and S_{th} are calculated as:

$$S_{el} = \frac{Q_{nom}}{Q_{ref} \cdot Vol} Y[U - V] \quad (8)$$

$$S_{th} = S_{el} \left[U - V - T \frac{dU}{dT} \right] \quad (9)$$

In Equations 8 and 9, Q_{nom} is the nominal capacity of the currently simulated battery, Q_{ref} is the capacity of the battery used to produce the reference discharge profiles, Vol is the current battery cell volume, V is the cell battery voltage and U, Y are functions derived by the model from the reference discharge profiles.

Since the CFD model setup requires a detailed knowledge of the battery cell material composition and electrochemistry, a preliminary calibration step has been performed, based on the reference 21700 LiNMC cell that has been thoroughly characterized in the experimental work of Waldmann et al. [11]. Table 3 collects the properties of each cell layer, which have been sourced from [11] and [12]–[14]. Note that properties are to be considered effective, taking into account the material porosity and the presence of the $LiFP_6$ electrolyte.
A 21x70 mm cylindrical domain has been realized, with Al and Cu metal caps at the positive and negative pole, respectively (Figure 5). Table 4 shows the equivalent properties that have been derived from the Table 3 data and applied to the electrochemically active cell domain, together with some of the main simulation parameters. As a first step, discharge curves at three different C-rates have been extracted from [11], to calibrate the electrochemistry-thermal coupling within the Fluent model. Figure 6 shows the coherence between the discharge curves that are automatically fitted by the software and the original experimental trends.

Table 3. Layer thicknesses and properties for the reference 21700 LiNMC battery cell [11]–[14].

Layer	Cathode	Anode	Collector (C)	Collector (A)	Separator
Material	NMC	Graphite	Al	Cu	PP
Thickness (μm)	125	126	20	10	16
Porosity (-)	0.29	0.48	-	-	0.5
ρ (kg/m³)	3749	1753	2719	8978	1119
C_p (J/kg K)	1009	1178	871	381	1680
λ (W/m K)	2.11	5.8	202	388	0.2
σ (siemens/m)	125	200	3.54e+7	5.8e+7	-

Table 4. Physical and numerical parameters adopted for the simulations of the reference 21700 LiNMC cell (properties referred to the cell active zone).

Parameter	Units	Value
Nominal capacity	*(Ah)*	2.457
Nominal voltage	*(V)*	3.6
Cut-off voltage (upper)	*(V)*	4.2
Cut-off voltage (lower)	*(V)*	2.7
ρ	*(kg/m^3)*	2764
C_p	*(J/kg K)*	1107
λ	*(W/m K)*	17.6
σ_+	*(siemens/m)*	1.256e+6
σ_-	*(siemens/m)*	1.028e+6
N. of computational cells	-	15360
Time step length	*(s)*	1
Time step sub-iterations	-	5

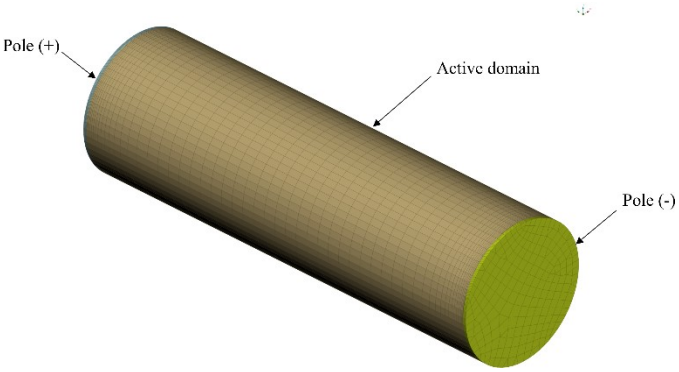

Figure 5. Representation of the computational domain adopted for the thermal simulations of the reference 21700 cell.

Thermal simulations have been subsequently performed, assuming a convective boundary condition at the external walls with a heat transfer coefficient (HTC) of 10 W/m^{2}K. The reference ambient temperature has been set to 25°C, as reported in the experiments. The HTC and ambient temperature are used to provide the correct heat flux at the boundaries, for the solution of the conductive energy equation (Eq. 5) within the battery solid domain.
Results are shown in Figure 7, in terms of the maximum temperature reached within the cell active domain during the discharge runs. The agreement between the simulations and experiments is generally good, with a slight temperature overestimation returned by the numerical predictions (up to about 10% at the highest C-rate).

It should be noted that several modeling uncertainties still persist, such as the effective value of the cell thermal capacity, as well as of the convective heat transfer coefficient. As such, the trend captured by the thermal modeling framework can be considered satisfactory and thus applicable to the main part of our study.

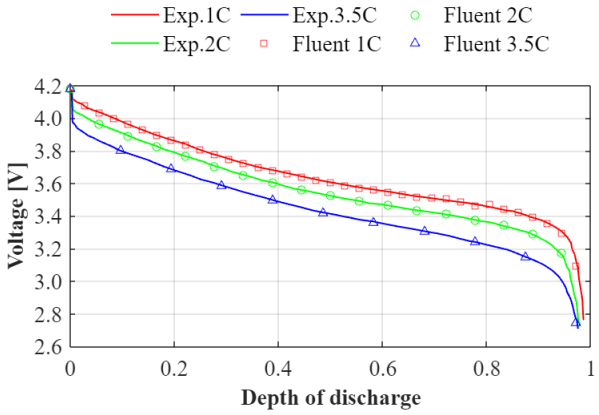

Figure 6. Discharge curves comparison for the reference 21700 test cell.

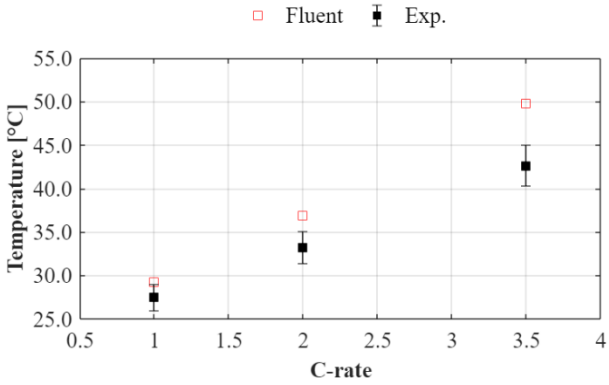

Figure 7. Maximum cell temperature comparison between Waldmann et al.'s experimental measurements and the 21700 test cell simulation.

Results and discussion

The comparison results between the two ECM models (Rint: n=0 and 3RC, n=3) at 25 °C for all tested cells and currents are shown in Figures 8-10. To quantify the difference between the experimental and estimated voltage, we used mean error analysis. The results reveal that at 1C both models perform well in terms of voltage vs. time at 25 °C.
The mean absolute error between model and experiment is below 1%. Further, as shown in Table 5, the simple 3RC model (n=3) based on the parameters predetermined by low current pulse test is relative better at 1C and can provide a higher accuracy than the Rint (n=0) model. This is expected because, apart from the SOC, the Rint

model is limited to purely ohmic response to a current pulse.
As can be seen from Figures 8-10, the major deviations are observed for 3C and 5C. In these cases model underestimates the real experimental values. Error is slightly reduced when using Rint model. Nevertheless, the voltage estimation accuracy is mostly below 10% in terms of mean error, which is comparable with the previously reported results [6], [15].

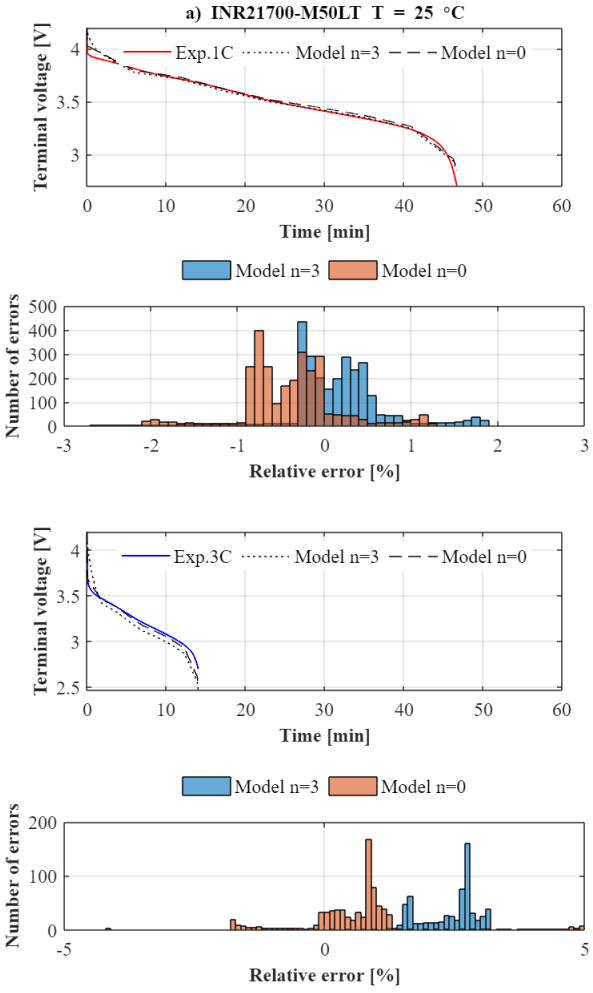

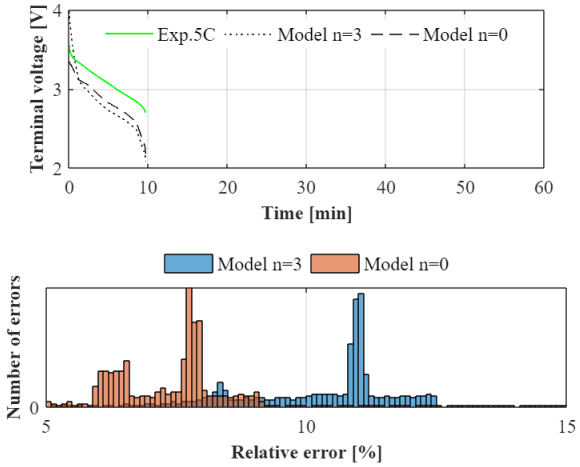

Figure 8. Comparison of the experimental and modelling discharge curves for the INR21700-M50LT at discharge rates of 1, 3 and 5 C and an environmental temperature of 25°C.

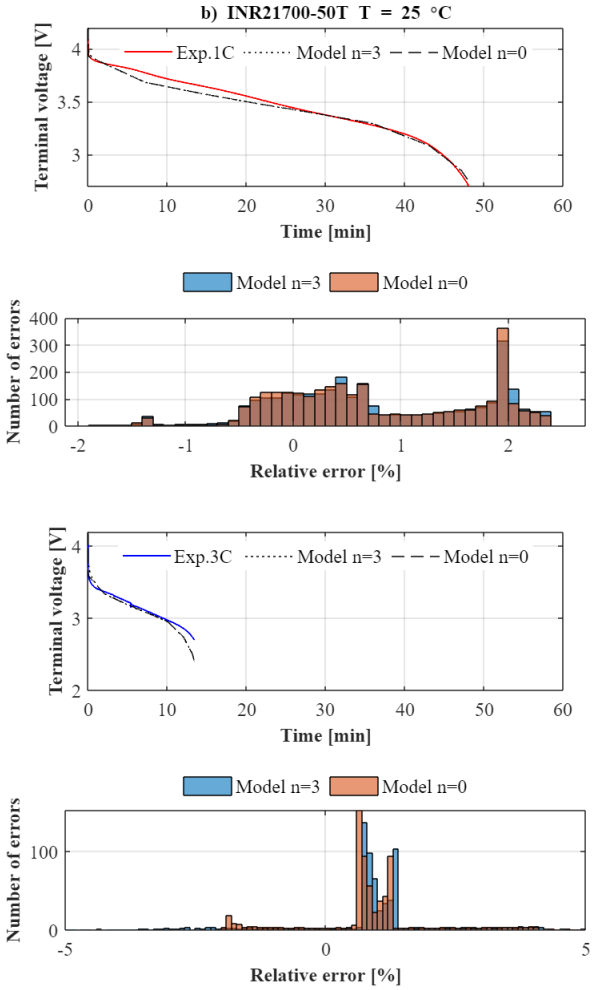

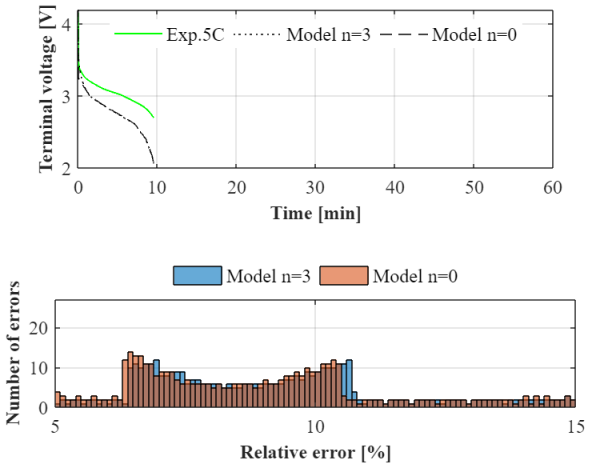

Figure 9. Comparison of the experimental and modelling discharge curves for the INR21700-50E at discharge rates of 1, 3 and 5 C and an environmental temperature of 25°C

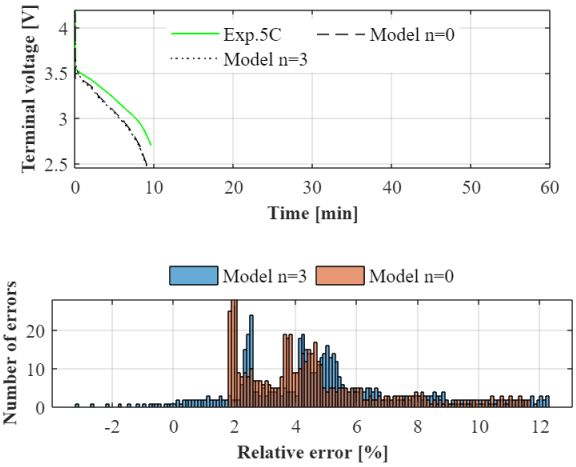

Figure 10. Comparison of the experimental and modelling discharge curves for the INR21700-40T at discharge rates of 1, 3 and 5 C and an environmental temperature of 25°C

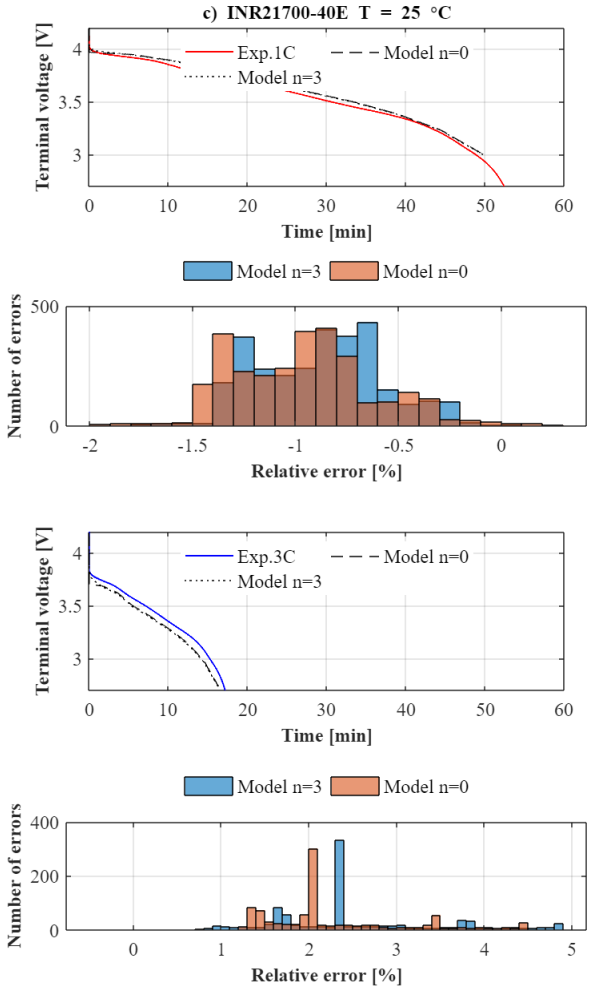

Table 5. Charging and discharging parameters of the cycle test.

Cell	Mean error[%]	Standard deviation[%]
INR21700-M50LT		
Model n=0		
1C	-0.45	0.74
3C	0.89	1.45
5C	7.86	2.57
Model n=3		
1C	0.03	0.91
3C	2.09	2.89
5C	9.54	5.51
INR21700-50E		
Model n=0		
1C	0.77	0.93
3C	1.48	2.27
5C	9.57	4.06
Model n=3		
1C	0.79	0.94
3C	1.48	2.47
5C	9.48	4.53
INR21700-40T		
Model n=0		
1C	-0.94	0.39
3C	2.30	0.84
5C	4.73	2.52
Model n=3		
1C	-0.87	0.32
3C	2.49	0.98

5C	5.03	2.91

Thermal simulations of the selected battery cells are also performed, based on the previously presented and validate Fluent modeling framework. Similarly to what previously shown, experimental discharge profiles produced from our laboratory measurements are directly used by the software to calculate thermal sources.

Figure 11 displays temperature vs. time profiles for the three investigated 21700 cells, comparing the experimental measurements with the Fluent thermal simulations performed to reproduce the static discharge tests. It should be noted that, in the absence of reliable data for the cell material composition and properties, the same battery simulation parameters previously adopted for the benchmark 21700 LiNMC cell have been applied here.

Results show a good agreement between the experiments and numerical predictions at 1C, for all the cells considered. At 3C, predictions are still in good accordance with measurements for the two larger capacity cells, while the profiles start to diverge for the INR21700-40T cell. The divergence increases at 5C, whereas only a slight discrepancy appears for the LGINR21700-M50LT and INR21700-50E cells towards the end of the discharge runs.

A possible explanation for the different behavior of the INR21700-40T cell is an inconsistency between the thermal properties of the benchmark 21700 LiNMC cell and the actual properties of the cell tested. In that regard, the specific heat capacity C_p is expected to have a major role, while at the highest C rates also a more accurate estimation of the convective heat transfer between the cells and the surrounding air is likely to be beneficial.

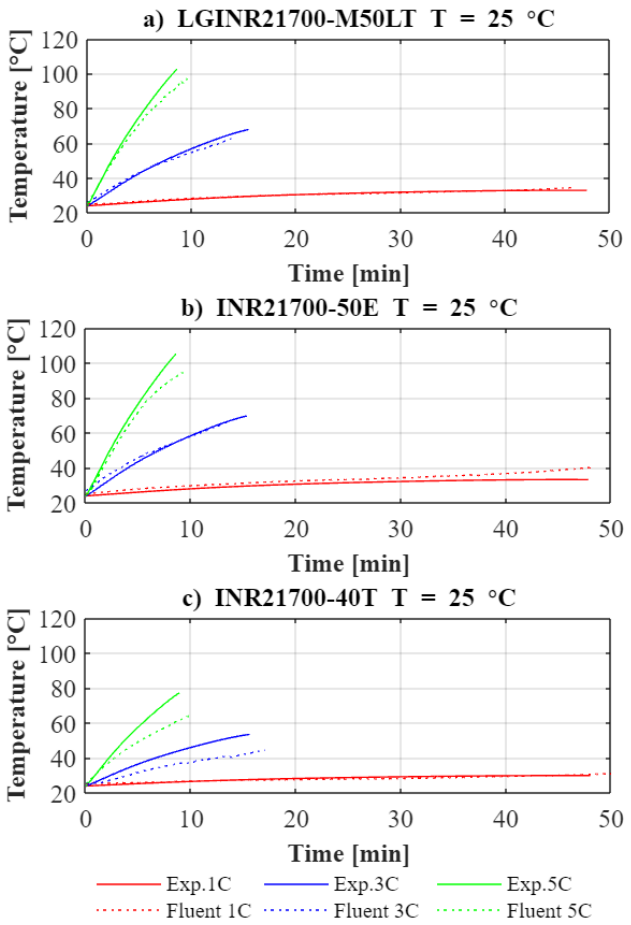

Figure 11. Temperature profiles obtained from the experiments and the Fluent thermal model for the a) LGINR21700-M50LT, b) INR21700-50E and c) INR21700-40T cells during discharge at 1, 3 and 5 C and with an environmental temperature of 25°C.

Conclusions

In the present paper, an ECM-based electrical model and a CFD-based thermal model have been developed for Li-ion NMC battery cells. The performances of both models have been compared against in-house experimental measurements made on three commercial 21700 NMC cells.
The results and analysis presented have demonstrated that the proposed combined approach has sufficient ability for both voltage and temperature predictions. The ECM-based method has shown a good potential for real time battery monitoring on board of electric vehicles and for other energy storage applications. The CFD-based method for thermal predictions has shown satisfactory accuracy, provided that a good estimate

for the cell battery thermophysical properties is available.
However, the terminal voltage-SOC relationship also changes with temperature, current and ageing. For the future work, the temperature and current effect on the model on battery temperature, SOC and voltage predictions will be investigated. Furthermore, a closer coupling between the developed electric model and multi-dimensional thermal simulation tools, such as the framework provided by the ANSYS® Fluent package, will be researched.

References

[1] "Global EV Outlook 2022 – Analysis - IEA." https://www.iea.org/reports/global-ev-outlook-2022 (accessed May 31, 2023).

[2] M. Dubarry, N. Vuillaume, and B. Y. Liaw, "From single cell model to battery pack simulation for Li-ion batteries," *J Power Sources*, vol. 186, no. 2, pp. 500–507, Jan. 2009, doi: 10.1016/J.JPOWSOUR.2008.10.051.

[3] Y. H. Chiang, W. Y. Sean, and J. C. Ke, "Online estimation of internal resistance and open-circuit voltage of lithium-ion batteries in electric vehicles," *J Power Sources*, vol. 196, no. 8, pp. 3921–3932, Apr. 2011, doi: 10.1016/J.JPOWSOUR.2011.01.005.

[4] C. Zhang, W. Allafi, Q. Dinh, P. Ascencio, and J. Marco, "Online estimation of battery equivalent circuit model parameters and state of charge using decoupled least squares technique," *Energy*, vol. 142, pp. 678–688, Jan. 2018, doi: 10.1016/J.ENERGY.2017.10.043.

[5] C. Zhang *et al.*, "A new design of experiment method for model parametrisation of lithium ion battery," *J Energy Storage*, vol. 50, p. 104301, Jun. 2022, doi: 10.1016/J.EST.2022.104301.

[6] Y. Hu, S. Yurkovich, Y. Guezennec, and B. J. Yurkovich, "A technique for dynamic battery model identification in automotive applications using linear parameter varying structures," *Control Eng Pract*, vol. 17, no. 10, pp. 1190–1201, Oct. 2009, doi: 10.1016/J.CONENGPRAC.2009.05.002.

[7] X. Hu, S. Li, and H. Peng, "A comparative study of equivalent circuit models for Li-ion batteries," *J Power Sources*, vol. 198, pp. 359–367, Jan. 2012, doi: 10.1016/J.JPOWSOUR.2011.10.013.

[8] *ANSYS® Academic Research CFD, Release 2020 R2, Fluent Theory Guide*. ANSYS Inc, 2020.

[9] G.-H. Kim, K. Smith, K.-J. Lee, S. Santhanagopalan, and A. Pesaran, "Multi-Domain Modeling of Lithium-Ion Batteries Encompassing Multi-Physics in Varied Length Scales," *J Electrochem Soc*, vol. 158, no. 8, p. A955, 2011, doi: 10.1149/1.3597614.

[10] U. Seong Kim, J. Yi, C. B. Shin, T. Han, and S. Park, "Modeling the Dependence of the Discharge Behavior of a Lithium-Ion Battery on the Environmental Temperature," *J Electrochem Soc*, vol. 158, no. 5, p. A611, 2011, doi: 10.1149/1.3565179.

[11] T. Waldmann, R. G. Scurtu, K. Richter, and M. Wohlfahrt-Mehrens, "18650 vs. 21700 Li-ion cells – A direct comparison of electrochemical, thermal, and geometrical properties," *J Power Sources*, vol. 472, Oct. 2020, doi: 10.1016/j.jpowsour.2020.228614.

[12] D. Werner, A. Loges, D. J. Becker, and T. Wetzel, "Thermal conductivity of Li-ion batteries and their electrode configurations – A novel combination of modelling and experimental approach," *J Power Sources*, vol. 364, pp. 72–83, 2017, doi: 10.1016/j.jpowsour.2017.07.105.

[13] E. J. Cheng, K. Hong, N. J. Taylor, H. Choe, J. Wolfenstine, and J. Sakamoto, "Mechanical and physical properties of LiNi0.33Mn0.33Co0.33O2 (NMC)," *J Eur Ceram Soc*, vol. 37, no. 9, pp. 3213–3217, Aug. 2017, doi: 10.1016/j.jeurceramsoc.2017.03.048.

[14] Y. H. Chen, C. W. Wang, X. Zhang, and A. M. Sastry, "Porous cathode optimization for lithium cells: Ionic and electronic conductivity, capacity, and selection of materials," *J Power Sources*, vol. 195, no. 9, pp. 2851–2862, May 2010, doi: 10.1016/j.jpowsour.2009.11.044.

[15] H. He, X. Zhang, R. Xiong, Y. Xu, and H. Guo, "Online model-based estimation of state-of-charge and open-circuit voltage of

lithium-ion batteries in electric vehicles," *Energy*, vol. 39, no. 1, pp. 310–318, Mar. 2012, doi: 10.1016/J.ENERGY.2012.01.009.

Contact Information

Dr. Barbara Mendecka,
barbara.mendecka@unicusano.it